Rhizosphere to the atmosphere: contrasting methane pathways, fluxes and geochemical drivers across the terrestrial-aquatic wetland boundary

Luke C. Jeffrey[1,2], Damien T. Maher[1,2,3], Scott Johnston[1], Kylie Maguire[1], Andrew D.L. Steven[4] and Douglas R. Tait[1,2].

[1]SCU Geoscience, Southern Cross University, PO Box 157, Lismore, NSW 2480, Australia.

[2]National Marine Science Centre, Southern Cross University, PO Box 4321, Coffs Harbour, NSW 2450, Australia.

[3]School of Environment, Science and Engineering, Southern Cross University, Lismore, NSW 2480, Australia

[4]CSIRO Oceans and Atmosphere, Queensland Biosciences Precinct, University of Queensland, 306 Carmody Rd, St Lucia, Brisbane 4067, Australia

Key Words:

Diffusion

Ebullition

Sediment redox

Coastal acid sulphate soils

Sulphate reduction

Iron reduction

Carbon cycle

Abstract

Although wetlands represent the largest natural source of atmospheric CH_4, large uncertainties remain regarding the global wetland CH_4 flux. Wetland hydrological oscillations contribute to this uncertainty, dramatically altering wetland area, water table height, soil redox potentials and CH_4 emissions. This study compares both terrestrial and aquatic CH_4 fluxes in permanent and seasonal remediated freshwater wetlands in subtropical Australia over two field campaigns, representing differing hydrological and climatic conditions. We account for aquatic CH_4 diffusion and ebullition rates, and plant-mediated CH_4 fluxes from three distinct vegetation communities, thereby examining diel and intra-habitat variability. CH_4 emission rates were related to underlying sediment geochemistry. For example, distinct negative relationships between CH_4 fluxes and both Fe(III) and SO_4^{2-} were observed. Where sediment Fe(III) and SO_4^{2-} were depleted, distinct positive trends occurred between CH_4 emissions and Fe(II) / acid volatile sulphur (AVS). Significantly higher CH_4 emissions ($p<0.01$) of the seasonal wetland were measured during flooded conditions and always during daylight hours, which is consistent with soil redox potential and temperature being important co-drivers of CH_4 flux. The highest CH_4 fluxes were consistently emitted from the permanent wetland (1.5 to 10.5 mmol m^{-2} d^{-1}), followed by the Phragmites australis community within the seasonal wetland (0.8 to 2.3 mmol m^{-2} d^{-1}), whilst the lowest CH_4 fluxes came from a region of forested Juncus sp. (-0.01 to 0.1 mmol m^{-2} d^{-1}) which also corresponded with the highest sedimentary Fe(III) and SO_4^{2-}. We suggest that wetland remediation strategies should consider geochemical profiles to help to mitigate excessive and unwanted methane emissions, especially during early system remediation periods.

1.0 Introduction

Wetlands are considered one of the most valuable ecosystems on Earth (Costanza et al., 2014) and may be classified as both permanently innndated (i.e lakes and shallow waters) and seasonally inundated (i.e. vegetated) biomes. They are biodiversity hotspots that provide ecosystem services such as water filtration, sediment trapping, floodwater retention and carbon (C) storage (Bianchi, 2007). Wetlands account for ~5.5% of terrestrial surfaces (Melton et al., 2013) and have been estimated to store from ~4% (Bridgham et al., 2014) to ~30% (Mitsch et al., 2013) of Earth's estimated 2500 Pg soil C pool (Lal, 2008). Pristine wetlands have long been considered net C sinks due to their high rates of productivity and low rates of decomposition (Petrescu et al., 2015); however due to their waterlogged nature and anaerobic soils, wetlands are ideal environments for the production of methane (CH_4), a potent greenhouse gas. As such, wetlands are recognised as Earth's largest natural source of CH_4 to the atmosphere (185 ± 21 Tg C yr^{-1}) (Saunois et al., 2016).

Resolving the drivers, pathways and effects of seasonal weather oscillations on wetland CH_4 sink or source behaviours is important to enable more accurate climate model projections and to reduce uncertainties in the global wetland CH_4 budget (Saunois et al., 2016;Kirschke et al., 2013). Weather oscillations affect the total wetland areal extent and inundation periods, with wet conditions facilitating anaerobic conditions favouring methanogenesis, while the opposite is seen during dry periods which potentially mitigates CH_4 emissions (Whiting and Chanton, 2001;Wang et al., 1996). Mitsch et al. (2013) estimated that the average ratio of freshwater wetland CO_2 sequestration to CH_4 emissions was 25.5:1, though this was later refuted by Bridgham et al. (2014). As CH_4 is 34 times more potent than carbon dioxide (CO_2) over a 100 year time scale (Stocker et al., 2013), this suggests that many freshwater wetlands may have a net positive radiative forcing effect on climate (Petrescu et al., 2015;Hernes et al., 2018). However, variability in geomorphology, wetland maturity, salinity and underlying geochemical composition all contribute to variable CH_4 dynamics (Bastviken et al., 2011;Mitsch and Gosselink, 2007;Poffenbarger et al., 2011;Whiting and Chanton, 2001). The lack of latitudinally-resolved wetland CH_4 emission data, the limited number of studies constraining the multiple wetland CH_4 flux pathways (i.e. ebullition, diffusion and plant-mediated) and the ongoing anthropogenic conversion of wetland systems (Saunois et al., 2016;Neubauer and Megonigal, 2015;Bartlett and Harriss, 1993) further contribute to the uncertainties around CH_4 regional to global scale budgets.

Extensive clearing and drainage of many coastal wetlands has occurred over the previous two centuries in order to accommodate agriculture, aquaculture and urban development (White et al., 1997;Armentano and Menges, 1986;Villa and Bernal, 2018). Drained wetlands can lead to rapid soil organic matter oxidation, and transform systems to net CO_2 sources (Deverel et al., 2016;Pereyra and Mitsch, 2018). Drainage systems can also reduce wetland inundation periods and alter sediment redox-dependant geochemistry and microbially-mediated reactions (Johnston et al., 2014), particularly those involving bioavailable iron (Fe(III)), sulphate (SO_4^{2-}) and nitrate (NO_3^-). Importantly, anaerobic carbon metabolism employing these terminal electron acceptors (Fe(III), SO_4^{2-}, NO_3^-) competes thermodynamically with methanogenic bacteria and archaea and thereby can inhibit CH_4 production (Burdige, 2012;Lal, 2008;Karimian et al., 2018;á Norði and Thamdrup, 2014). With increasing value placed on the ecosystem services provided by wetlands, many degraded systems are now undergoing remediation and re-flooding (Johnston et al., 2014). However, the ecosystem benefits, such as enhanced biodiversity and water quality, may come at a price in the form of high initial CH_4 flux rates, and predicted net radiative forcing for several centuries post-remediation - thus posing a 'biogeochemical compromise' (Hemes et al., 2018).

Within Australia, it has been estimated that more than 50% of natural wetlands have been lost to land use change, drainage and degradation since European settlement (Finlayson and Rea, 1999;ANCA, 1995). By comparing and reviewing pristine Australian wetland carbon stocks to drained sites, and GHG dynamics, Page and Dalal (2011) estimated that through biomass loss, enhanced soil respiration, N_2O production and a reduction in CH_4 emissions, that Australian wetland loss equated to ~1.2 Pg CO_2 equivalents emitted to the atmosphere. Much of eastern Australia's freshwater coastal wetlands are underlain by Holocene derived sulphidic sediments (i.e. pyrite – Fe_2S, known as coastal acid sulphate soils; CASS) formed during periods of higher sea levels (White et al., 1997;Walker, 1972). When CASS are drained, pyrite is oxidised, producing sulphuric acid (H_2SO_4). This results in highly acidic soils with pH levels as low as 3 (Sammut et al., 1996;Johnston et al., 2014). After rainfall events, groundwater transports H_2SO_4 from the CASS landscapes into nearby creeks and estuaries (Sammut et al., 1996). The low pH groundwater discharge also mobilises iron and aluminium, fuels aquatic deoxygenation, and can lead to large fish kills and degradation of infrastructure (White et al., 1997;Johnston et al., 2003;Jeffrey et al., 2016;Wong et al., 2010). Drained CASS wetlands typically contain abundant reactive Fe(III) and exhibit complex sulphur and Fe cycling (Burton et al., 2006;Boman et al., 2008;Burton et al., 2011). Wetland iron and sulphur cycling can

profoundly influence CH_4 production and consumption via a series of complex redox reactions coupled with organic matter mineralisation (Holmkvist et al., 2011;Sivan et al., 2014). As such, terminal electron acceptor availability is critical when considering wetland remediation and the biogeochemical compromise paradigm.

Here we assess CH_4 emissions from a remediated freshwater CASS wetland in subtropical eastern Australia, and compare fluxes from the permanent wetland and the adjacent seasonal wetland ecotypes. We hypothesize that wetland CH_4 emissions will differ significantly between the campaigns and between the four wetland communities due to differences in soil chemistry, hydrology and plant physiology. We account for three atmospheric flux pathways for methane; ebullition, diffusion and plant-mediated fluxes, over diel cycles and within different hydrological conditions. CH_4 fluxes were also assessed in relation to the underlying soil properties, including sulphate, reactive iron III and iron II, acid volatile sulphur, chloride and organic carbon.

2.0 Methods

2.1 Study site

Cattai Wetland is located on the mid-coast of New South Wales, Australia. The reserve covers 500 hectares, featuring a shallow permanent wetland covering an area of approximately 16 hectares that is adjacent to a seasonal wetland and floodplain located to the south (Fig. 1). Both sites discharge into the nearby Coopernook Creek, a tributary of the larger Manning River estuary. The site was extensively cleared and low-lying areas drained during the early 1900's in order to aid agriculture and development in the region. As a result of this anthropogenic drainage, the oxidation of CASS produced sulphuric acid and episodic acidic discharge to adjacent creeks for many years (Tulau, 1999). To ameliorate acidic discharge, the natural hydrology of the site was restored in 2003 through the decommissioning of agricultural drains and removal of floodgates. Re-flooding of the CASS landscape has reduced the production of sulphuric acid, acid discharge and aluminium and iron mobilisation, hence improving the downstream water quality (GTCC, 2014).

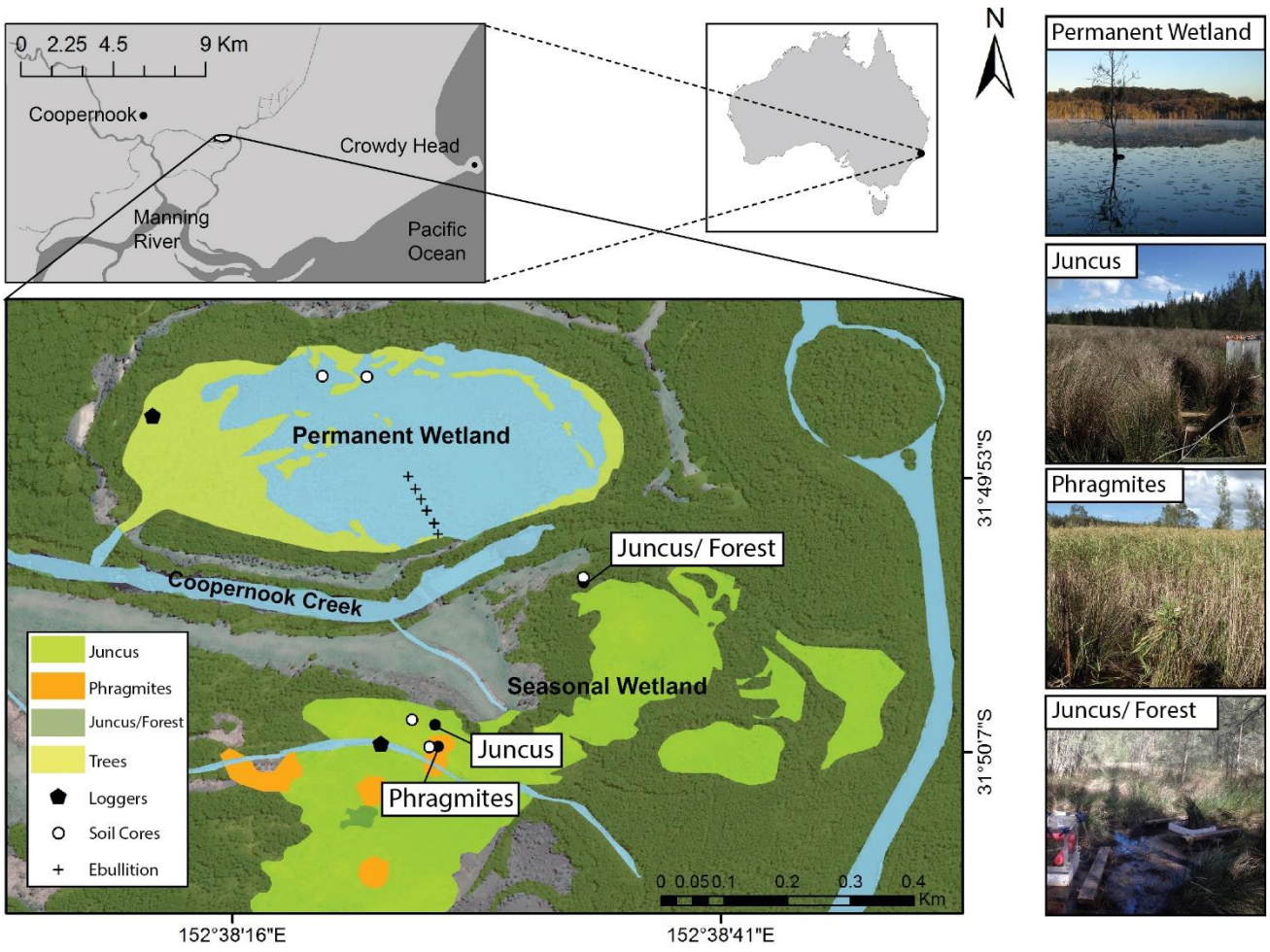

144

145 **Fig. 1** The seasonal wetland study sites consisting of Juncus (*Juncus kraussii*), Phragmites
146 (*Phragmites australis*), Juncus/ Forest (*Juncus kraussii* below *Casuarina sp.*) and the
147 permanent wetland indicating sediment coring sites, ebullition replicate transect, 24 h
148 vegetation time series sites and imagery of vegetation ecotypes.

149 The region receives a mean annual rainfall of 1180 mm with the majority falling during
150 early autumn with an average maximal monthly rainfall occurring in March (152 mm). The
151 lowest rainfall generally occurs during the winter months with average minimal rainfall during
152 September (60 mm). Average minimum and maximum summer temperatures range from 17.6
153 °C to 29 °C (January) and in winter range from 5.9 °C to 18.5 °C (July) (BOM, 2018). The
154 dominant vegetation type within the permanent wetland is an introduced waterlily species
155 (*Nymphaea capensis*), while the fringes of the wetland consist of wetland tree species;
156 *Casuarina* sp. and *Melaleuca quinquenervia*. The seasonal wetland to the south is dominated
157 by the sedge; *Juncus kraussii* ('Juncus' from herein) and features scattered stands of

158 *Phragmites australis* ('Phragmites' from herein) with areas of slightly higher elevation
159 dominated by *Juncus kraussii* below *Casuarina sp.* ('Juncus/ Forest' from herein) (Fig. 1).

160

161 **2.2 The aquatic CH_4 flux of the permanent wetland**

162 To quantify CH_4 ebullition rates, up to 12 ebullition domes were deployed during two
163 different hydrological conditions (detailed below) at ~20 m intervals along a longitudinal
164 transect, from the edge of the permanent wetland towards the centre. Each dome was carefully
165 suspended below the water level by flotation rings, ensuring minimal disturbance of sediment
166 and the water column. Gas samples were extracted from the headspace of each dome using a
167 300 mL gas tight syringe at periods of ~48 h. The volume was recorded and each sample then
168 diluted using ambient air (1:729 ratio) and analysed in situ using a using a manufacturer
169 calibrated cavity ring-down spectrometer (Picarro G2201-*i*) to determine CH_4 concentrations
170 (ppm). Diffusive CH_4 fluxes from the permanent wetland were measured using a floating
171 chamber with a portable greenhouse gas analyser (UGGA, Los Gatos Research). To account
172 for spatial and temporal variability, measurements were conducted during both day-time and
173 night-time, and sampling within vegetated areas featuring lilies (*Nymphaea capensis*); that
174 were only present during the second campaign, forested areas (*Melaleuca* sp.) and in areas
175 where no aquatic vegetation was present (i.e. open water). A total of 39 CH_4 floating chamber
176 incubations averaging ~8 minutes in duration were recorded over the two campaigns, with 19
177 during C1 (nine at night) and 30 during C2 (12 at night). The average r^2 value of linear
178 regressions of CH_4 concentrations versus time during chamber incubations was 0.97 ± 0.05.
179 One chamber measurement was disregarded as an outlier (as it was more than three times the
180 standard deviation of the mean) and any chambers capturing ebullition bubbles (determined by
181 a nonlinear increase in concentration) were also disregarded. Examples of these, in addition to
182 the ebullition and diffusive CH_4 flux methods and measurements from the permanent wetland
183 have previously been reported elsewhere (Jeffrey et al., 2019).

184

185 **2.3 Plant-mediated CH_4 fluxes**

186 Simultaneous time series chamber experiments were conducted over a minimum of 24
187 hours to measure diel CH_4 fluxes during each campaign from the three different wetland
188 vegetation ecotypes. These ecotypes were *Juncus kraussii*, *Phragmites australis* and *Juncus*

kraussii amongst *Casuarina sp.* forest (Fig. 1). In each ecotype, three acrylic bases (65 x 65 x 30 cm) were installed four months before the first time series experiment, to minimise disturbance to the sediment profile and vegetative rhizosphere. Vegetative flux chambers were constructed of an aluminium frame with clear Perspex walls and roof that matched the areal footprint of the pre-inserted acrylic bases. The chambers were 100 cm, 150 cm and 50 cm high for at Juncus, Phragmites and Juncus/Forest sites respectively. The custom sizes were tailored for the different vegetation heights, whilst minimising chamber volume as much as possible. Each chamber was leak-tested under laboratory conditions prior to fieldwork.

Before each field incubation, chambers were flushed with atmospheric air then carefully lowered over the vegetation and onto the acrylic base ensuring an air tight seal. A small fan circulated internal air within each chamber. Air within the chamber was pumped through a closed loop from the top of the chamber using gas tubing (Bevaline), passing through a drying agent (Drierite desiccant) and then analysed in situ using a calibrated cavity ring-down spectrometers (Picarro G2201-*i* or LosGatos), recording the flux rate of CH_4 (ppm/sec). The gas flow was returned near the base inside each vegetation chamber closing the loop. Vegetation incubation times ranged from 6 to 15 minutes depending on the flux rate and were taken from triplicate chambers to account for heterogeneity within each ecotype. During the first time-series (C1), an average of 16.7 ± 2.9 daytime flux measurements (i.e. after sunrise) and 7.3 ± 1.6 night time (i.e. after sunset) were recorded within each habitat. During the second campaign (C2) an average of 27.7 ± 2.9 (day time) and 10.3 ± 1.5 (night time) flux measurements were recorded within each habitat. In addition, CH_4 fluxes from the adjacent exposed soils or shallow overlying water at each site were also measured at ~4 hourly intervals to determine the influence and role of plant-mediated CH_4 fluxes compared to non-vegetated CH_4 fluxes. Light and temperature loggers (Onset Hobo) measured the changes in diel air temperature (°C) and photosynthetically active radiation (PAR) at each site.

2.4 Soil geochemistry and redox conditions

A water logger (Minidiver) was deployed in the permanent wetland before the first campaign to monitor changes in water depth (cm) and temperature (°C). Field pH (pH_F) and the redox potential (Eh_F; reported against standard hydrogen electrode) were determined in situ, by directly inserting the electrode into the soils (5 cm depth, 8 replicates) at each site. A composite sampling approach (3 cores) was used to collect sediment samples from each site,

to determine organic C content, $Fe(III)_{HCl}$, $Fe(II)_{HCl}$, Cl, SO_4^{2-} and acid volatile sulphur (AVS). The cores were sampled in close proximity to the time series habitats (5 to 15 m) in December 2016, but within the permanent wetland the cores were taken from elsewhere to avoid disturbance of the shallow water column and sediments. The cores were extracted by inserting a 4.0 cm diameter acrylic tube into the sediment to a depth of up to 50 cm. Cores were immediately sectioned into 2 cm increments to a depth of 20 cm, and 5 cm increments thereafter, ensuring higher vertical resolution in the organic rich near-surface sediments. Samples were immediately placed into air-tight bags, then frozen within 12 hr of collection at -16°C in a portable freezer and transferred to -80°C freezer in the laboratory.

For analysis, the frozen samples were thawed in an oxygen-free anaerobic chamber (1-5% H_2 in N_2), using an oxygen consuming palladium (Pd) catalyst. The defrosted samples were homogenised using a plastic spatula. AVS content was determined by adding 1-2 g of wet sediment with 6 M HCl:1 M L-ascorbic acid. The liberated H_2S was captured in 5 ml of 3% Zn acetate in 2 M NaOH and then quantified using iodometric titration. The reactive Fe fractions were determined using a sequential extraction procedure optimised for acid sulphate soils based on Claff et al. (2010). Poorly crystalline solid-phase Fe (II) and Fe (III) were determined by extracting 2 g wet sub-samples with cold N_2-purged 1 M HCl for four hours. Aliquots of 0.45 µm-filtered extract were analysed for Fe (II) [$Fe(II)_{HCl}$] and total Fe [Fe_{HCl}] using the 1,10-phenanthroline method with the addition of hydroxylammonium chloride for total Fe (APHA, 2005). The Fe(III) [$Fe(III)_{HCl}$] was determined by the difference of [Fe_{HCl}] – [$Fe(II)_{HCl}$]. Total organic carbon (TOC) and total S (S_{Tot}) were determined via a LECO CNS-2000 carbon and sulphur analyser. Chloride and sulphate concentrations were measured using filtered (0.45 µm) aliquot from a 1:5 water extract of freshly defrosted wet soil, as per Rayment and Higginson (1992) via ion chromatography using a Metrosep A Supp4-250 column, an RP2 guard column and eluent containing 2 mM $NaHCO_3$, 2.4 mM Na_2CO_3 and 5% acetone, in conjunction with a Metrohm MSM module for background suppression.

2.5 Calculations

Both the air-water and vegetative CH_4 fluxes were calculated for the chamber deployments in the permanent wetland and seasonal wetland using the equation:

$$F = (s(V/RT_{air}A))t \quad (1)$$

where *s* is the regression slope for each chamber incubation deployments (ppm sec^{-1}), *V* is the chamber volume (m^3), *R* is the universal gas constant (8.205 x 10^{-5} m^3.atm.K^{-1}.mol^{-1}), T_{air} is the air temperature inside the chamber (*K*), *A* is the surface area of the chamber (m^2) and *t* is the conversion factor from seconds to day, and to mmol. We assume that atmospheric pressure is 1 atm. Ebullition rates (E_b) (mmol m^{-2} d^{-1}) were calculated using the equation*:*

$$E_b = ([CH_4].CH_{4Vol.})/ A.V_m.Td \quad (2)$$

where $[CH_4]$ is the CH_4 concentration in the collected gas (%), $CH_{4Vol.}$ is the gas volume sampled (L), A is the funnel area (m^2), V_m is the molar volume of CH_4 at in situ temperature (L) and Td is deployment time (days).

2.6 Statistical analysis

As the CH_4 flux data was non-parametric we used a Kruskal-Wallis one way analysis of variance (ANOVA) on ranks to test for significant differences between each campaign, between flux pathways and between diel variability, where $p<0.001$. Dunn's multiple pairwise comparisons were then used to analyse specific sample pairs ($p<0.05$).

3.0 Results

Prior to the first campaign in April 2017 (C1), an extreme hot/drying summer period occurred (Fig. 2). This resulted in an average wetland water column temperature of 23.3 ± 0.7 ºC and a water depth in the permanent wetland as low as ~7.3 cm, with exposed sediments along the wetland perimeter during the preceding month. There was a high rainfall event prior to C1 with 342 mm of rainfall recorded over the preceding two weeks and an additional 35 mm of rain occurring during C1 fieldwork (Fig. 2) thus raising the water column depth in the permanent wetland to 77.2 cm in less than four weeks. This C1 deployment was therefore categorized as the 'post-dry/flooded' period, where air temperatures ranged from 13.3 to 22.8 ºC and the average water column temperature in the permanent wetland was 20.4 ± 0.5 ºC. The second fieldwork campaign was conducted in September 2017 (C2) under cool/drying conditions, where air temperatures ranged from as low as 3.4 ºC to 34.9 ºC (Fig. 2), with cooler average water temperatures 12.6 ± 0.4 ºC in the permanent wetland (Fig. 2). The depth of the permanent wetland at this time had dropped slightly to ~33 cm (Fig. 2).

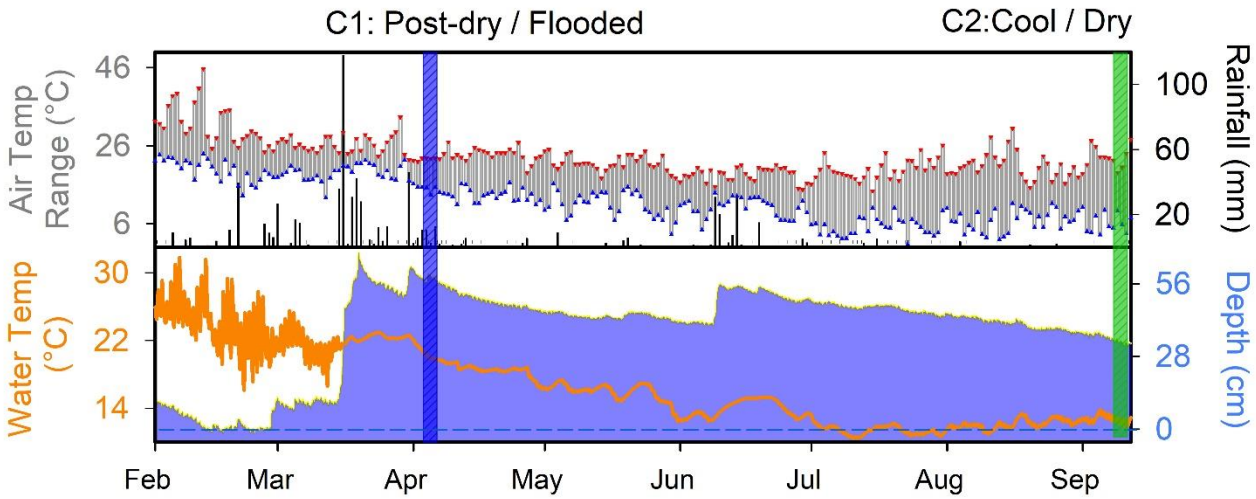

Figure 2. Hydrograph for the seven months of 2017 indicating daily rainfall, maximum/ minimum air temperature, water temperature and antecedent hydrology. Vertical coloured bands represent the two fieldwork campaigns.

3.1 Sediment core profiles and soil redox potentials

Average concentrations from soil cores (Table 1, Fig. 3) were based upon the top 20 cm of the profile, where the highest organic carbon concentrations were found. The $Fe(III)_{HCl}$ concentrations were greater than $Fe(II)_{HCl}$ at all three seasonal wetland sites, however the permanent wetland showed an opposite trend with low concentrations of both Fe(III) (5.6 ± 10.7 mmol kg^{-1}) and SO_4^{2-} (1.5 ± 1.0 mmol kg^{-1}) (Fig. 3, Table 1). The highest average concentrations of $Fe(III)_{HCl}$ were found at the Juncus/ Forest site (204.0 ± 51.6 mmol kg^{-1}) and highest and similar concentrations of SO_4^{2-} were in Phragmites and Juncus/ Forest sediments (45.4 ± 41.0 mmol kg^{-1} and 43.3 ± 16.7 mmol kg^{-1}) (Fig. 3, Table 1). Net positive redox potential was found at all four sites during C1 (under post-dry/ flooded conditions) indicating a lag time between recent flooding and the onset of reducing conditions. In contrast, a negative redox potential was found within the permanent wetland and Phragmites during C2, indicating reduced conditions under cool drying conditions (Table 1). The TOC concentrations (%) were highest in the upper profiles and similar across all sites (Fig. 3, Table 1) averaging 13.4 ± 7.6%.

Table 1. Summary of plant-mediated CH_4 fluxes from the seasonal wetland time series and diel CH_4 diffusive fluxes and ebullition from the permanent wetland during C1 (post-dry/

303 flooded) and C2 (cool/ drying). The corresponding sediment core data are average
304 concentrations from 0 to 20 cm below ground level.

CH_4 flux (mmol m^{-2} d^{-1})	Ebullition	Diffusion	Juncus	Phragmites	Juncus/ Forest
Sediment flux - C1			0.06	0.04	0.10
Day time - C1		0.57	1.79	2.64	0.13
Night time - C1		2.07	1.50	1.59	0.10
Daily average - C1	2.02	1.49	1.70	2.27	0.12
Sediment flux - C2			0.00	0.20	0.00
Day time - C2		11.72	0.06	0.94	0.13
Night time - C2		8.39	0.04	0.48	0.10
Daily average - C2	2.10	10.46	0.05	0.77	-0.01
FeHCl (II) (mmol kg-1)	202.3		11.6	15.4	1.5
FeHCl (III) (mmol kg-1)	5.6		83.3	56.1	204.0
SO42- (mmol kg-1)	1.5		17.6	45.4	43.3
Cl:SO42-	14.8		8.4	13.9	7.4
AVS (µmol g-1)	18.5		0.7	0.9	0.3
TOC (% C)	11.6		14.3	14.8	14.6
C1 - Redox Eh (mV)	71.7		46.5	9.6	54.4
C2 - Redox Eh (mV)	-216.3		11.9	-89.3	424.5

305

306

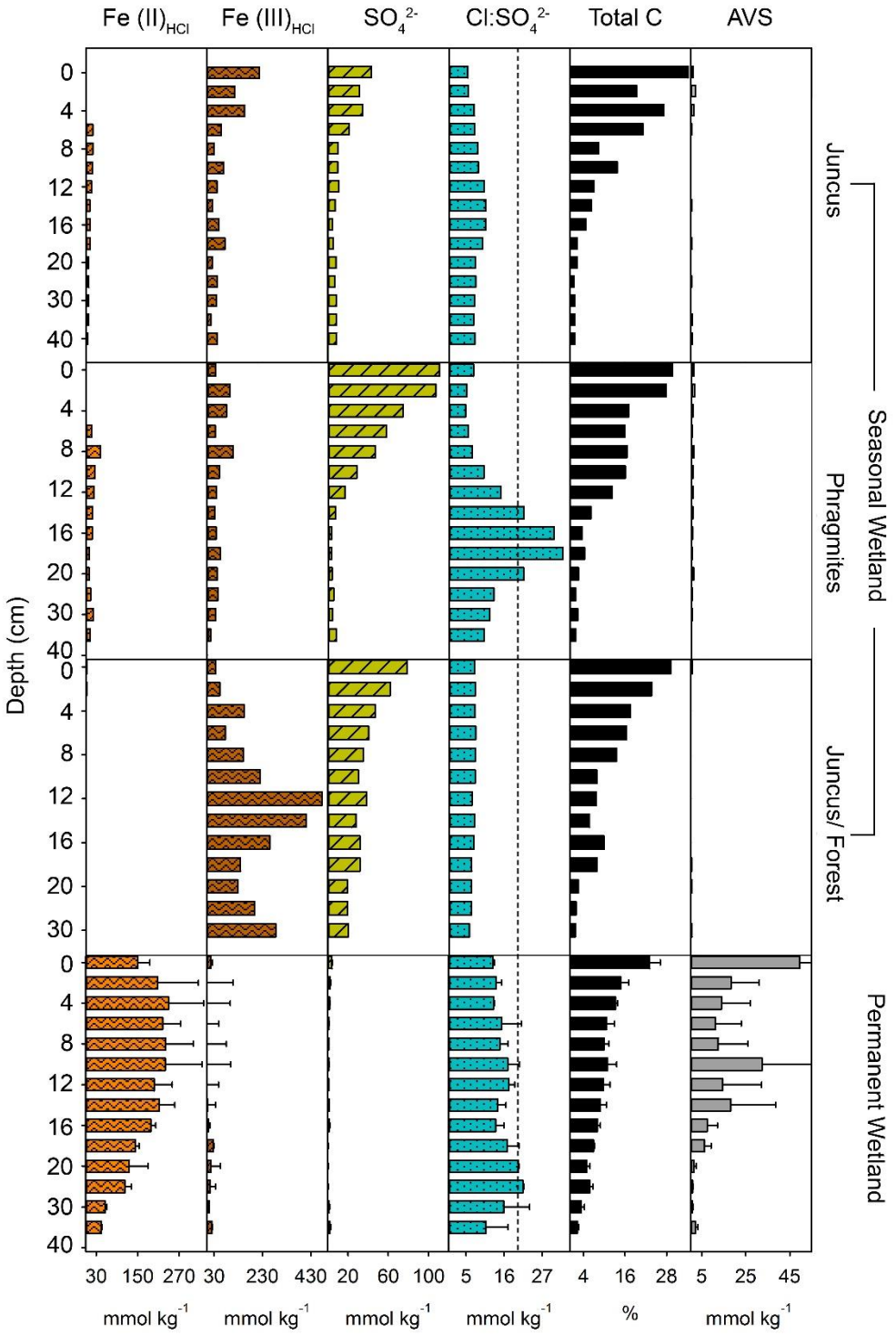

307

308 **Figure 3.** Soil profiles of the permanent and seasonal wetland sites indicating $Fe(II)_{HCl}$,
309 $Fe(III)_{HCl}$, SO_4^{2-}, $Cl:SO_4^{2-}$ (a proxy for depletion of marine-derived sulphate, where >20 is
310 broadly indicative of SO_4^{2-} reduction and <8 CASS pyrite oxidation (Mulvey, 1993), total C

and acid volatile sulphur (AVS). Note: The permanent wetland profiles are averages from two adjacent sites with error bars representing the standard deviation.

3.2 Permanent and Seasonal Wetland CH_4 fluxes

The vegetation time series revealed diel variability of plant-mediated CH_4 emissions occurred at most ecotypes, with the highest CH_4 fluxes occurring during daytime around mid-day and the lowest CH_4 fluxes during the night time (Fig. 4, Table 1). The lowest CH_4 fluxes were found in Juncus/ Forest habitat with a net negative CH_4 flux observed during C2 time series. The CH_4 sediment fluxes measured amongst each vegetation time series were consistently much lower than the plant-mediated CH_4 fluxes indicating that the vegetation was indeed the main conduit for CH_4 to the atmosphere (Fig. 4, Table 1). The CH_4 fluxes were highly variable between the replicates at each site. Temperature and PAR followed similar diel trends to each other and had positive correlations to CH_4 emissions (Fig. 4).

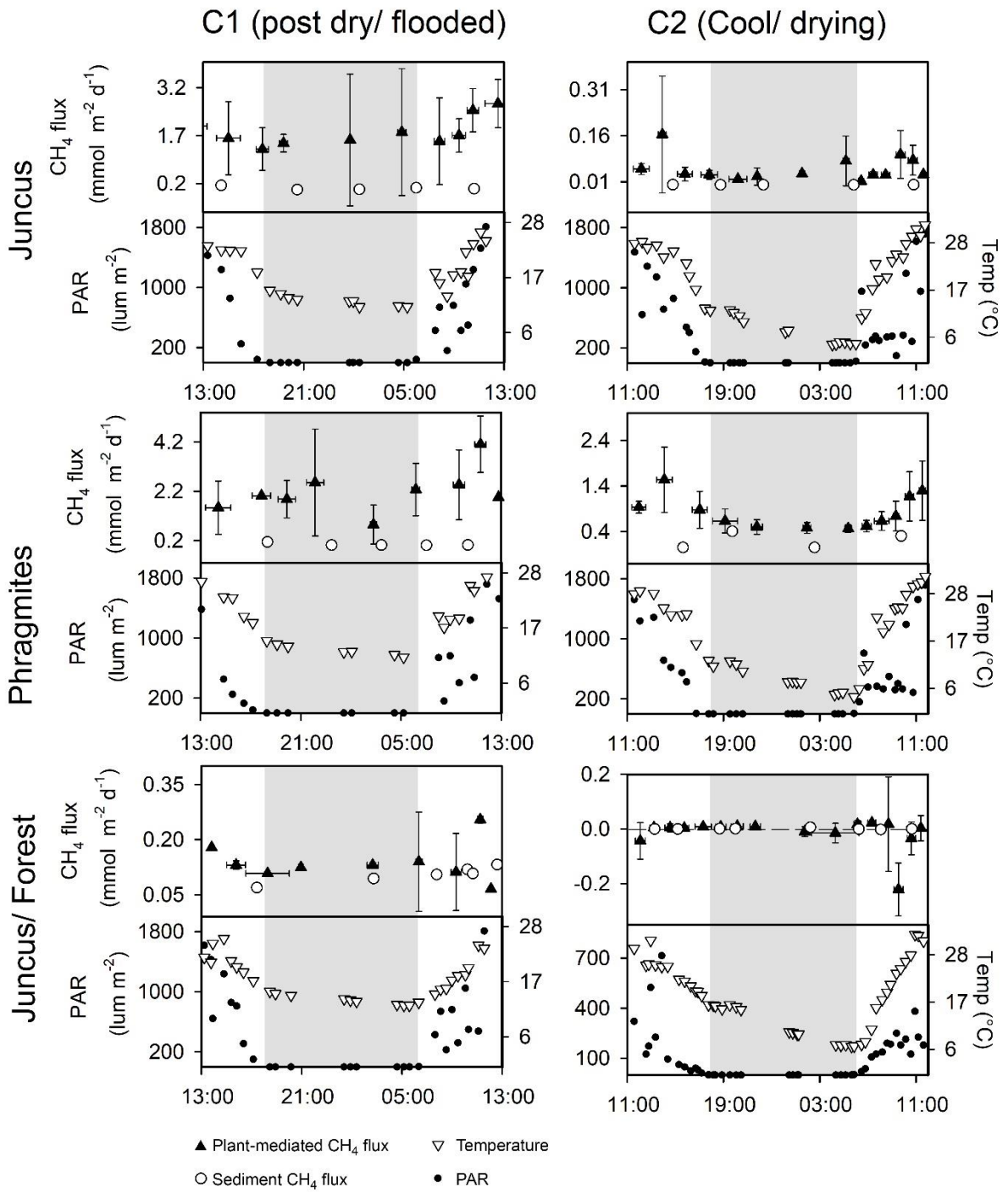

325

326 **Figure 4.** Simultaneous 24 h time series of vegetative CH_4 fluxes from the seasonal wetland
327 ecotypes at Cattai Wetland during C1: post-dry/flooded (Apr 2017) and C2: cool/drying
328 conditions (Sep 2017). The vertical error bars of the plant-mediated CH_4 flux (mmol m^{-2} d^{-1})
329 represent standard deviation of the triplicate time series measurements taken from each site and
330 horizontal bars represent the total aggregated time period represented by replicate chambers.

The grey shading indicates night-time. Note: Different y-axis scales for CH_4 to highlight diel trends.

CH_4 fluxes from the three vegetation types were significantly higher during C1 than during C2 ($p<0.001$). During C1, the CH_4 fluxes from the Juncus and Phragmites were not significantly different from each other but were both significantly higher ($p<0.001$) than Juncus/Forest however, during C2 the CH_4 fluxes of each seasonal wetland habitat were significantly different between all habitats ($p<0.05$) (Fig. 5). The highest average CH_4 fluxes in each of the vegetation types always occurred during the daytime but were not significantly different to night time fluxes (Fig. 5, Table 1). Phragmites consistently emitted the highest CH_4 fluxes (2.27 ± 1.42 mmol m^{-2} d^{-1} during C1 and 0.77 ± 0.46 mmol m^{-2} d^{-1} during C2). The Juncus/ Forest ecotype within the seasonal wetland consistently produced the lowest CH_4 fluxes of all sites, with a negligible flux that was not significantly different from zero occurring during C2 (-0.01 ± 0.08 mmol m^{-2} d^{-1}).

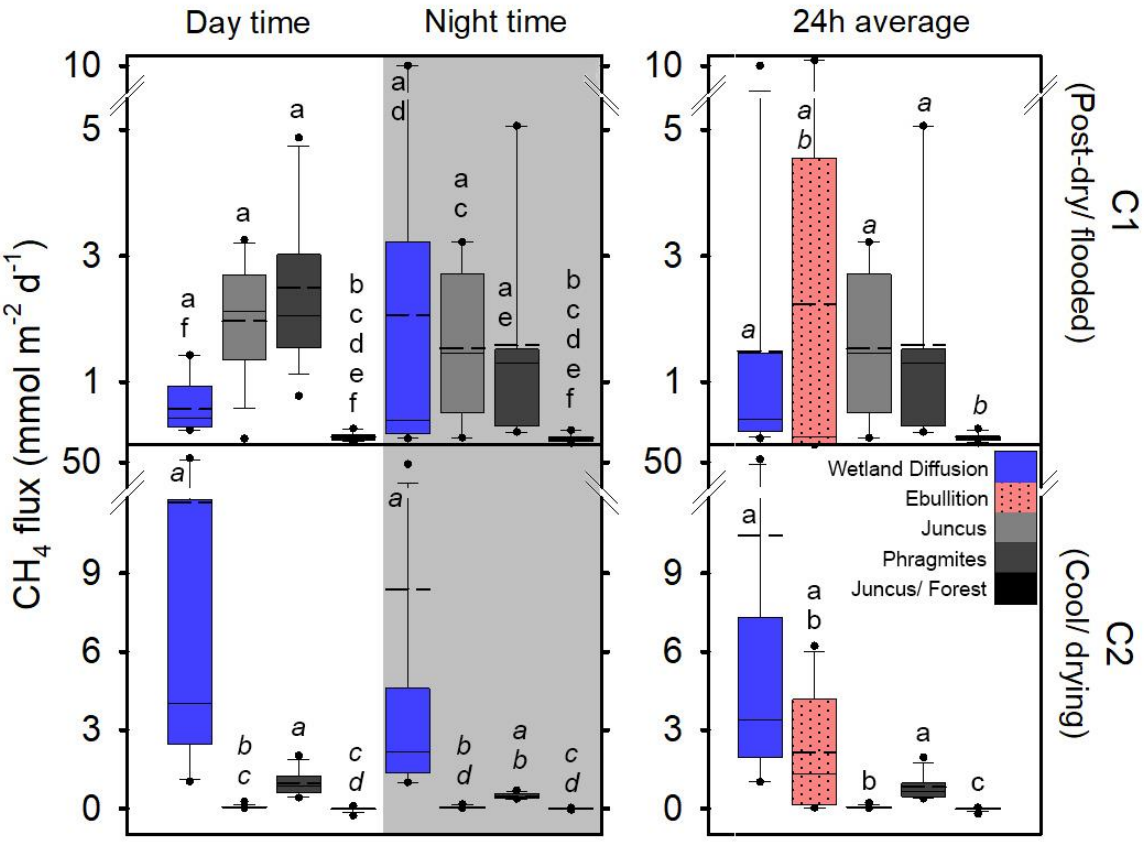

Figure 5. Fluxes of CH_4 from diel sampling and ebullition over two campaigns from the permanent wetland and adjacent 24 h time series of the seasonal wetland vegetation types.

348 Note: Diffusive fluxes during C2 include chambers featuring lilies, dashed line represents the
349 average, solid line represents the median and dots represent 5^{th} and 95^{th} percentiles. Letters
350 show groups that did not differ significantly ($p>0.05$) using ANOVA on ranks and Dunn's
351 pairwise comparisons within each campaign.

352

353 The permanent wetland showed an inverse trend with seven-fold and significantly
354 higher ($p<0.001$) diffusive fluxes during the cool/drying C2 when lilies were present (10.46 ±
355 15.81 mmol m^{-2} d^{-1}) compared to the post-dry/flooded C1 when no lilies were present (1.49 ±
356 2.75 mmol m^{-2} d^{-1}), while the ebullition rates were similar during both campaigns (Fig. 5, Table
357 1). Overall, the diffusive fluxes of the permanent wetland were within range of CH_4 fluxes
358 from the three seasonal wetland habitats but were significantly higher than Juncus/Forest
359 during both campaigns, and Juncus during C2 (Fig. 5). Diel diffusive flux variability was not
360 significant between day time and night time (Table 1, Fig. 5).

361

362 **3.3 Temperature and PAR**

363 Correlation plots for both temperature (ºC) and sunlight (PAR) versus CH_4 emissions
364 from the three vegetation ecotypes showed no distinct relationships with the exception of
365 Phragmites during C2 for PAR (r^2=0.18, $p<0.01$) and temperature (ºC) (r^2=0.35, $p<0.001$). No
366 clearer trends were observed by combining all site measurements, nor separating daytime
367 fluxes and drivers from night time fluxes and drivers.

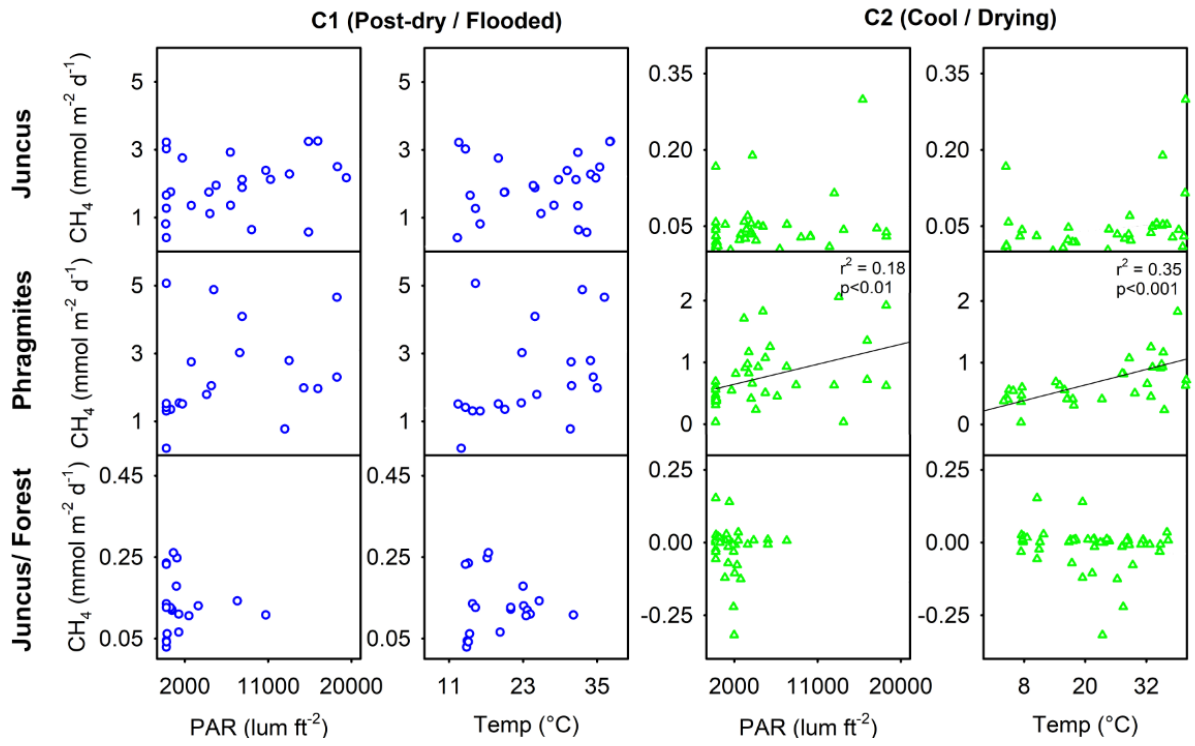

Figure 6. Correlations of CH_4 with temperature (ºC) and photo-synthetically active radiation (PAR) (lum ft^{-2}) for the three wetland vegetation sites of Cattai Wetland during two field campaigns.

4.0 Discussion

4.1 Geochemistry of the CASS landscape

Sediment profiles provide insights to the historical geochemical changes that have occurred across the CASS landscapes of the four Cattai Wetland sites (Fig. 3). We base our results and discussion on the upper rhizosphere depth zone (20 cm) as this featured the highest organic carbon concentrations and is therefore assumed to be an active area of carbon metabolism, and CH_4 production and consumption (Nedwell and Watson, 1995). If we assume that relatively uniform deposition of late Holocene materials occurred, the differences between present day profiles are related to historical changes in hydrology and land use, topographic elevation, geochemical trajectories and vegetative carbon inputs. For example, the permanent wetland shows distinct differences to the adjacent seasonal wetland sites, with divergent geochemical signatures of both iron and sulphate that reflect the sustained inundation (Table 1, Fig 5). The permanent wetland had significantly lower Fe(III) ($p<0.001$) and 11 to 30 fold lower SO_4^{2-} concentrations within the upper soil profile compared to the seasonal wetland. The

ratio of $Fe(III)_{HCl}$ to $Fe(II)_{HCl}$ from the flooded soils of the permanent wetland was 0.03, indicating the sediments were almost completely depleted of Fe(III). Under reducing conditions where there is low SO_4^{2-} and little to no Fe(III) to competitively exclude methanogenesis, CH_4 production becomes more favourable. Indeed, CH_4 production was on average highest from the permanent wetland, especially when considering the duel CH_4 pathways of ebullition and air-water diffusion (Table 1).

In addition to sulphate reduction, some depletion of the sulphur pool from the permanent wetland may have occurred due to drainage exports of sulphuric acid (H_2SO_4) discharging from the CASS landscape throughout the last century. Alternatively, reducing conditions induced by re-flooding freshwater wetlands is known to encourage the re-formation of AVS and pyrite (FeS_2) and produce alkalinity, thereby attenuating acid production and discharge (Burton et al., 2007;Johnston et al., 2012;Johnston et al., 2014) and reducing the total SO_4^{2-} pool of CASS landscapes. While the AVS concentrations found within the permanent wetland (up to 18.5 µmol g^{-1}) were a result of sulphate reduction induced by CASS wetland restoration, they nonetheless represent a relatively volatile form of sulphur, which is at risk of rapid oxidation during drought periods (Johnston et al., 2014;Karimian et al., 2017). The AVS concentrations of the permanent wetland sites were more than 20-fold higher than the three adjacent seasonal wetland sites, and represent a potentially volatile by-product and consequence of re-flooding CASS soil landscapes, in addition to leading to increases of CH_4 emissions (Table 1).

The soil profile from the seasonal wetland Juncus/ Forest habitat featured abundant $Fe(III)_{HCl}$ (with an $Fe(III)_{HCl}$ to $Fe(II)_{HCl}$ ratio of 136) and also SO_4^{2-}. This was associated with the lowest fluxes of CH_4 for both sampling periods (Fig. 3, Table 1). Relatively low CH_4 fluxes from Juncus/ Forest are likely due to the more oxidising conditions present at this site and the surfeit of thermodynamically favourable terminal electron acceptors (i.e. Fe(III) and SO_4^{2-}), which would competitively exclude organic matter degradation by methanogenic archaea (Postma and Jakobsen, 1996). At the other seasonal wetland sites, the average Fe(III) and SO_4^{2-} concentrations were intermediate, (i.e. lower than Juncus/ Forest, but higher than the permanent wetland), although in the upper profile the Phragmites had more SO_4^{2-} while Juncus had more Fe(III) (Fig. 3, Table 1). CH_4 flux values from these sites were also intermediate (Table 1). Sediment profiles from both Juncus and Phragmites indicated a degree of Fe reduction based on the ratio of Fe(III):Fe(II) which were 7.2 and 3.6 respectively. The redox potentials from Phragmites during both C1 and C2 campaigns (9.6 mV and -89.0 mV respectively) were

consistently lower than Juncus during C1 and C2 campaigns (46.5 mV and 12.0 mV respectively), which is consistent with the more reducing conditions encouraging CH_4 production in Phragmites habitat. Further, as iron reduction yields more free energy than SO_4^{2-} reduction (Burdige, 2012), then Fe reduction at the Juncus site may outcompete CH_4 production ahead of SO_4^{2-} reduction in Phragmites, which may help explain some of the differences in CH_4 production between the two sites. The positive significant trends between Fe(II), AVS and the $Cl:SO_4^{2-}$ ratios with CH_4 flux rates (r_s=0.88, p<0.01) further support our hypothesis that reducing conditions and a smaller pool of sediment Fe(III) and SO_4^{2-} facilitate higher CH_4 production rates (Fig. 7). Alternatively, the negative trends observed between soil redox potentials, SO_4^{2-}, Fe(III) and CH_4 fluxes affirm that the abundance of thermodynamically favourable terminal electron acceptors play a role in attenuating CH_4 production at each site.

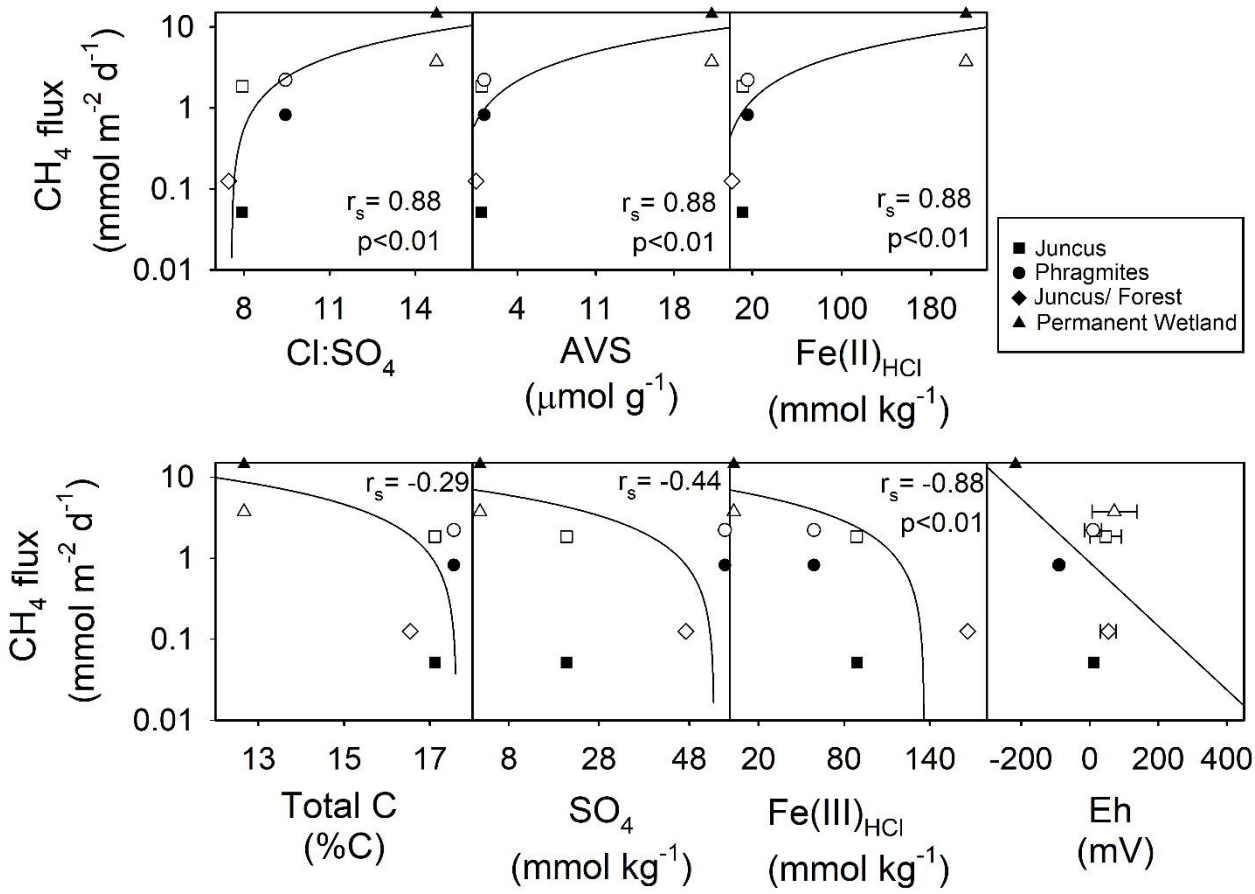

Figure 7. Regression analysis of average daily CH_4 fluxes (mmol m^{-2} d^{-1}) vs subsoil parameters of 0-20 cm core depth (i.e. CH_4 'active' zone). Note: Log scale y-axis of CH_4 fluxes from the four wetland ecotypes over two campaigns. Note: The r_s values were calculated using Spearman rho are for C1 (black shapes) and C2 (white shapes).

4.2 Plant-mediated CH_4 fluxes from the seasonal wetland

Plant-mediated CH_4 fluxes were significantly higher ($p<0.001$) during C1 under post-dry/flooded conditions with 20-30 cm of standing waters in the seasonal wetland (Table 1). While waterlogged conditions are an obvious driver of higher CH_4 production rates from saturated sediments in addition to the geochemical differences (previously discussed), other drivers which may explain these trends include differences in diel variability in temperature, PAR and plant physiology, which may influence CH_4 gas transport pathways.

In vegetated seasonal wetlands, plant-mediated gas transport is recognised as a dominant pathway for CH_4 emission to the atmosphere and accounts for up to 90% of total wetland fluxes (Sorrell and Boon, 1994;Whiting and Chanton, 1992). For plant survival in near-permanent inundation environments, oxygen transport occurs via the aerenchyma downwards to the rhizome. This increases the plant performance by mitigating (i.e. oxidising) the accumulation of phytotoxins such as sulphides and reducing metal ions around the roots (Armstrong and Armstrong, 1990;Armstrong et al., 2006;Penhale and Wetzel, 1983). As oxygen transfer to the rhizosphere occurs, an exchange of sedimentary CH_4 can be efficiently transported from the rhizosphere to atmosphere, bypassing sedimentary oxidative processes along the way. This process in plants can be either convective (i.e. pressurised) or via passive diffusive gas flow, both of which are adaptive traits of many wetland species (Konnerup et al., 2011;Armstrong and Armstrong, 1991).

During both campaigns the highest CH_4 fluxes from seasonal wetland vegetation were emitted from Phragmites and always occurred during daylight (Table 1, Fig. 8). In *Phragmites australis*, the presence of pressurised lacunar leaf culms drive a mass flow of oxygen to the rhizome and back to the atmosphere via older (non-pressurised) efflux culms (Sorrell and Boon, 1994;Henneberg et al., 2012). This process has been widely studied in wetlands featuring *Phragmites australis*, as it is one of the most productive and wide spread flowering wetland species (Clevering and Lissner, 1999;Brix et al., 2001;Chanton et al., 2002;Tucker, 1990). Milberg et al. (2017) found no apparent diel patterns of CH_4 fluxes from *Phragmites australis* during seven campaigns within the Swedish growing season. In a mid-latitude prairie wetland, Kim et al. (1998) showed that CH_4 emissions peaked around midday and that daytime emissions were about 3-fold higher than night time emissions, positively correlating with temperature and PAR. These were similar to our findings with highest CH_4 fluxes of each time series occurring near midday (4.88 mmol m^{-2} d^{-1} at 10:50 am during C1 and 2.06 mmol m^{-2} d^{-}

469 [1] at 12:15 pm during C2) (Fig. 4). We also found a positive significant relationship between
470 CH_4 flux and both temperature and PAR during C2 (Fig. 6). The often high diel variability in
471 CH_4 fluxes from *Phragmites australis* occurs as convective gas transport increases rhizospheric
472 oxygen and CH_4 exchange via living culms during the daytime, whereas molecular diffusion
473 during the night time facilitates a more passive and lower CH_4 flux pathway through dead
474 culms (Chanton et al., 2002;Armstrong and Armstrong, 1991).

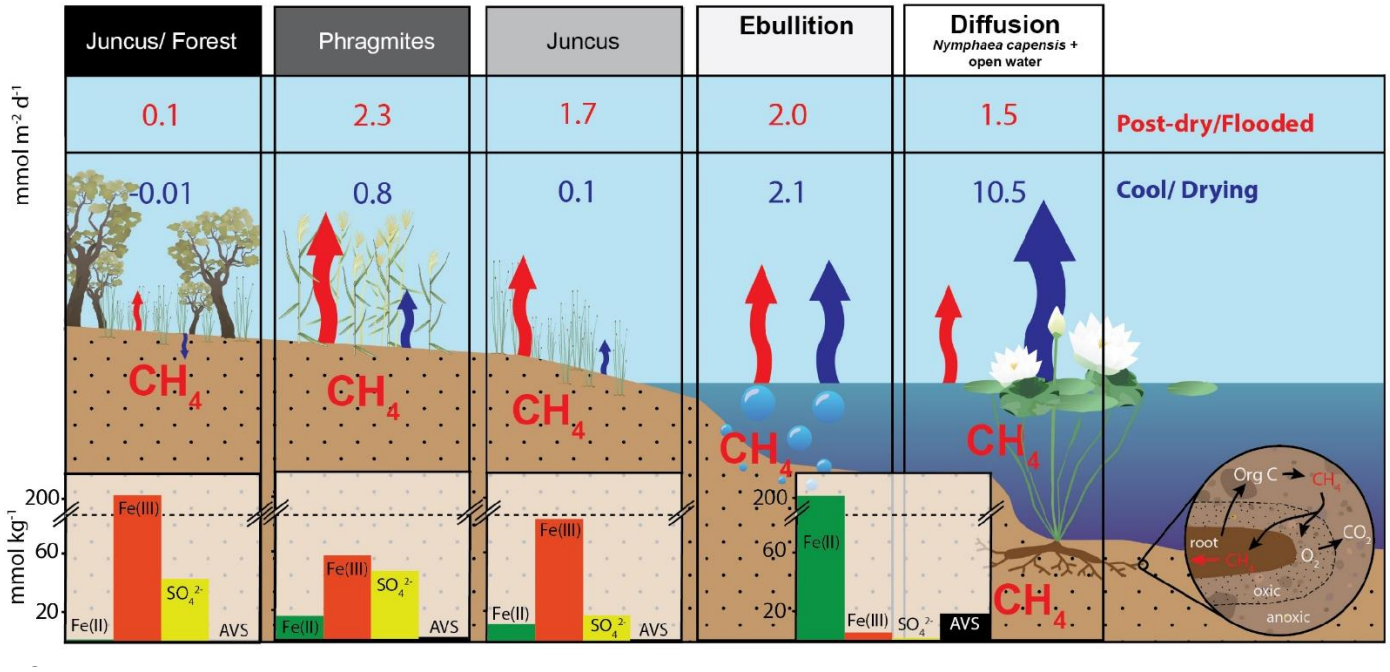

476 **Figure 8.** Conceptual model summarising the terrestrial and aquatic CH_4 fluxes (mmol m^{-2} d^{-1})
477 and sediment core profile parameters (mmol kg^{-1}) of the permanent and seasonal wetlands
478 during C1 (post-dry/flooded conditions) and C2 (cool/drying conditions) of Cattai Wetland.
479 Conceptual diagram rhizome process insert adapted from (Conrad, 1993). Note: Dashed line
480 highlights y-axis break.

481

482 One possible reason CH_4 fluxes were lower from Juncus than Phragmites despite their
483 close geographical location, may be due to the passive gas diffusion mechanism utilised by
484 *Juncus sp*. (Henneberg et al., 2012). Unlike the pressurised conductive gas flow mechanisms
485 of Phragmites, many wetland rush species (such as *Juncus sp.*) employ passive diffusive gas
486 flow to survive within water logging environments (Konnerup et al., 2011;Brix et al., 1992).
487 Despite diffusion being a less efficient gas transport mechanism (Konnerup et al., 2011), plant-
488 mediated CH_4 diffusion is recognised as the dominant pathway for CH_4 emissions from many

seasonal wetland species. During C1 and C2, day time fluxes (diffusive) from Juncus were only 19% and 33% higher than night time fluxes (diffusive). In comparison, from Phragmites these day:night ratios were almost triple this (67% and 94% higher) during the same periods. This may potentially be due to the more efficient daytime conductive gas transfer pathway of CH_4 through *Phragmites australis* compared to the more passive diffusive CH_4 gas transfer pathway of *Juncus kraussii* and/or the effectiveness of these different species to alter sedimentary redox conditions. This suggests that non-pressurized pathways may result in lower net rhizosphere-atmosphere gas exchange of CH_4 from seasonal wetland vegetation. Alternatively, root depth and root density differ between these two species (Moore et al., 2012;De La Cruz and Hackney, 1977), which may further influence redox dynamics in the rhizosphere, and the potential extent of net gas exchange.

The Juncus/ Forest habitat emitted significantly lower fluxes of CH_4 during both time series campaigns and was a net sink for CH_4 during C2 (Table 1, Fig. 8). Although wetland trees have recently been shown to contribute significantly to CH_4 fluxes from flooded environments (Pangala et al., 2017), we could not quantify or constrain the role of trees as a conduit of methane to the atmosphere at this site. Regardless, there were clearly lower CH_4 fluxes through the *Juncus kraussii* at the Juncus/ Forest habitat compared to the Juncus only habitat. As the species at ground level were identical, these differences are not related to vegetative gas transport mechanisms, nor organic carbon content (Table 1). Shading by the overhanging trees may inhibit the daytime diffusive CH_4 gas transport through Juncus/ Forest habitat assumable to lower rates of photosynthesis, however PAR was only lower during C2 (Fig. 7) and so does not appear to explain the CH_4 flux differences observed during C1. The differences are therefore likely explained by the higher positive redox potentials (Table 1) that may be partially attributable to rhizome aeration by the nearby trees, and more abundant thermodynamically favourable terminal electron acceptors (i.e. Fe(III) and SO_4^{2-}) (Fig. 3) all of which can inhibit methane production within the sediments (Burdige, 2012).

4.3 Permanent Wetland CH_4 fluxes

Diffusive CH_4 fluxes from the permanent wetland varied considerably between campaigns; however, ebullition fluxes were similar (Table 1, Fig. 8). The highest CH_4 fluxes for both ebullition and diffusion (2.1 mmol m^{-2} d^{-1} and 10.5 mmol m^{-2} d^{-1} respectively) occurred during C2 despite cooler conditions (Fig. 2. Fig. 8). This however was the opposite trend to the

seasonal wetland CH_4 fluxes (Table 1, Fig. 8). One reason may be due to the antecedent hydrological conditions before C1 (Fig. 2). Jeffrey et al. (2019) reported that a water level drawdown of the permanent wetland after a hot and drying summer period exposed some of the permanent wetland sediments to oxidative conditions. This may have oxidised a portion of the labile sedimentary carbon pool prior to C1 sampling of the permanent wetland, therefore reducing the total CH_4 pool observed during C1 sampling. A lag time (ranging from weeks to months) for recovery of the CH_4 pool post-drought has been observed in other systems (Boon et al., 1997) and also during lab-based experiments (Knorr et al., 2008; Freeman et al., 1992). Further, during C2 the return of macrophyte species *Nymphaea caspensis* most likely enhanced CH_4 gas transport from the rhizosphere to the floating chambers, as discussed in detail in Jeffrey et al. (2019). Therefore this combination of drivers most likely explain the higher CH_4 fluxes during C2 when the system (and lilies) had sufficient time to recover, despite lower water column temperatures that would normally reduce microbial metabolism rates. This hypothesis is also supported by the shift of net positive redox potential of the permanent wetland during C1 (71.7 ± 65 mV), to a strong negative redox potential during C2 (-216 ± 42 mV) indicating that there was a time lag for reducing conditions to recover within the permanent wetland for C2. Further, although aquatic vegetation can facilitate root zone aeration therefore increasing sedimentary redox potentials, as no aquatic vegetation was present in the permanent wetland during C1, this suggests that water level drawdown was the main driver of the observed redox conditions. This highlights the critical role of antecedent hydrological conditions and how dynamic weather oscillations of drought and floods (a common occurrence of many Australian wetland systems), strongly influence the redox potentials, soil geochemistry and ultimately CH_4 fluxes.

4.4 Implications and conclusions

Within the global wetland CH_4 budget, both subtropical systems and southern hemisphere systems are poorly represented (Bartlett and Harriss, 1993;Bastviken et al., 2011) (Fig. 9). Further, the fluxes from seasonal wetlands are poorly constrained (Pfeifer-Meister et al., 2018) due to their intermittent nature and variability of intra-seasonal areal extent, which may compound why natural wetlands have the largest uncertainty of the global methane budget (Saunois et al., 2016;Kirschke et al., 2013). Although the temporal resolution of our study cannot be up scaled to realistic annual estimates, our high resolution sampling strategy

provided insights to daily CH_4 flux rates revealing distinct differences between different vegetation types across the terrestrial aquatic wetland boundary. Our CH_4 emissions rates were at the low end of the scale of measurements made in southern hemisphere subtropical systems but within range of northern hemisphere subtropical systems of similar latitudes (Fig. 9).

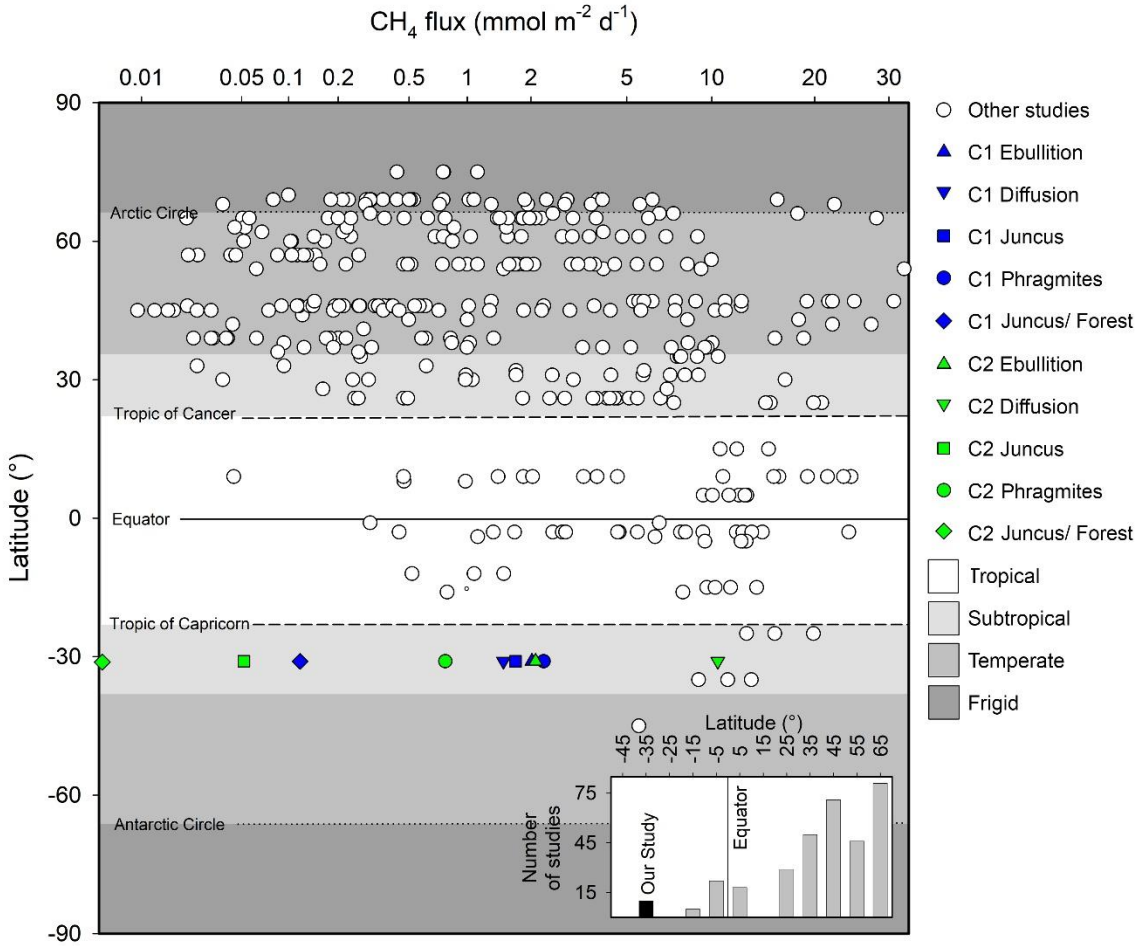

Figure 9. Summary of major CH_4 wetland reviews by Bartlett and Harriss (1993), Bastviken et al. (2011) and modelled fluxes by Cao et al. (1998) adapted from Jeffrey et al. (2019) highlighting latitudinal trends and bias from a variety of wetland systems. Inset figure highlights number of studies in these reviews by latitudinal increments of 10° poleward of the equator. Note: x axis scaled to highlight subtle differences between studies.

Although remediating degraded wetlands through re-flooding is a common technique to improve biodiversity, increase C sequestration and improve downstream water quality issues (Johnston et al., 2014;Johnston et al., 2004), our results propose a nuanced dilemma for land

use managers, as wetland remediation can potentially have net positive radiative forcing effects on the Earth's climate due to high rates of CH_4 production (Petrescu et al., 2015). This has also been shown to be particularly high during early remediation periods (Hemes et al., 2018). Our results suggest that seasonal wetlands emit less CH_4 on an areal basis than permanent wetlands, yet carbon accumulation in these soils may be lower (Brown et al., 2019). Longer-term studies over annual cycles encompassing seasonal drivers and CH_4 fluxes would further test this hypothesis of the different drivers between seasonal and permanent wetland systems.

Our results also suggest that selective hydrological restoration of wetlands featuring sediments with abundant thermodynamically favourable terminal electron acceptors (i.e. Fe(III) or SO_4^{2-}) may be a (partial) biogeochemical solution (also suggested by Hemes et al. (2018)) to both remediate degraded sites whilst simultaneously mitigating some CH_4 emissions. When Fe(III) and SO_4^{2-} are abundant in anaerobic environments they provide preferential terminal electron acceptors for microbial metabolism and thus limit methanogenesis via competitive exclusion (Achtnich et al., 1995). However, high rates of sulphate reduction coupled with Fe reduction can also lead to the accumulation of metal sulphide minerals e.g. pyrite and AVS (Johnston et al., 2014). Under permanently saturated and low oxygen conditions, metal sulphides will steadily accumulate and remain relatively benign. However, if the saturated state of remediated sites cannot be maintained, AVS may react with oxygen resulting in undesirable production of acidity and low pH conditions. Therefore the remediation of wetlands for carbon storage should involve careful site selection to both limit CH_4 production and to avoid redox related geochemical by-products with detrimental environmental effects.

This study has highlighted how sediment geochemistry is intimately related to CH_4 production and consumption. While high sulphate and Fe(III) favour lower CH_4 production, sites featuring more reducing conditions and depleted sulphate and Fe(III) favour the highest CH_4 fluxes. Results reveal distinct differences between the areal CH_4 fluxes of four different eco-types located within a remediated subtropical Australian wetland and indicate high variability between campaigns. By combining novel and well established techniques we delineated several CH_4 pathways of both seasonal and permanent wetland sources (ebullition, diffusion and plant-mediated pathways) and linked these to hydrological drivers. This provided evidence that soil geochemistry is an important factor to consider for wetland remediation in the context of CH_4 production and mitigation strategies. The CH_4 emissions results were

comparable to other wetlands of similar latitudes and contribute important data for both the understudied southern hemisphere wetlands and seasonal subtropical wetland ecotypes.

Acknowledgements

We would like to thank to Roz Hagan, Bob McDonnell, Zach Ford for assistance in the field. We also thank Roz Hagan for processing the sediment cores, Isaac Santos and Ceylena Holloway for technical support and Mid Coast Council for assistance. LCJ acknowledges postgraduate support from CSIRO. This work was supported by funding from the Australian Research Council. Graphic components used in conceptual model courtesy of the Integration and Application Network, University of Maryland Centre for Environmental Science (www.ian.umces.edu/symbols).

References

á Norði, K., and Thamdrup, B.: Nitrate-dependent anaerobic methane oxidation in a freshwater sediment, Geochimica et Cosmochimica Acta, 132, 141-150, 2014.

Achtnich, C., Bak, F., and Conrad, R.: Competition for electron donors among nitrate reducers, ferric iron reducers, sulfate reducers, and methanogens in anoxic paddy soil, Biology and Fertility of Soils, 19, 65-72, 1995.

ANCA: Issues paper for the Wise use Workshop, 4–6 December. Wetlands and migratory Wildlife Unit of the Australian Nature Conservation Agency, Canberra. 42 pp, 1995.

Armentano, T., and Menges, E.: Patterns of change in the carbon balance of organic soil-wetlands of the temperate zone, The Journal of Ecology, 755-774, 1986.

Armstrong, J., and Armstrong, W.: Light-enhanced convective throughflow increases oxygenation in rhizomes and rhizosphere of Phragmites australis (Cav.) Trin. ex Steud, New Phytologist, 114, 121-128, 1990.

Armstrong, J., and Armstrong, W.: A convective through-flow of gases in Phragmites australis (Cav.) Trin. ex Steud, Aquatic Botany, 39, 75-88, 1991.

Armstrong, J., Jones, R., and Armstrong, W.: Rhizome phyllosphere oxygenation in Phragmites and other species in relation to redox potential, convective gas flow, submergence and aeration pathways, New Phytologist, 172, 719-731, 2006.

Association, A. P. H., Association, A. W. W., Federation, W. P. C., and Federation, W. E.: Standard methods for the examination of water and wastewater, American Public Health Association., 1915.

Bartlett, K. B., and Harriss, R. C.: Review and assessment of methane emissions from wetlands, Chemosphere, 26, 261-320, 1993.

Bastviken, D., Tranvik, L. J., Downing, J. A., Crill, P. M., and Enrich-Prast, A.: Freshwater methane emissions offset the continental carbon sink, Science, 331, 50,2011.

Bianchi, T. S.: Biogeochemistry of estuaries, Oxford University Press New York, 2007.

Boman, A., Åström, M., and Fröjdö, S.: Sulfur dynamics in boreal acid sulfate soils rich in metastable iron sulfide—the role of artificial drainage, Chemical Geology, 255, 68-77, 2008.

Boon, P. I., Mitchell, A., and Lee, K.: Effects of wetting and drying on methane emissions from ephemeral floodplain wetlands in south-eastern Australia, Hydrobiologia, 357, 73-87, 1997.

Bridgham, S. D., Moore, T. R., Richardson, C. J., and Roulet, N. T.: Errors in greenhouse forcing and soil carbon sequestration estimates in freshwater wetlands: a comment on Mitsch et al. (2013), Landscape Ecology, 29, 1481-1485, 2014.

Brown, D. R., Johnston, S. G., Santos, I. R., Holloway, C. J., and Sanders, C. J.: Significant organic carbon accumulation in two coastal acid sulfate soil wetlands, Geophysical Research Letters, 0, 10.1029/2019gl082076, 2019.

Brix, H., Sorrell, B. K., and Orr, P. T.: Internal pressurization and convective gas flow in some emergent freshwater macrophytes, Limnology and Oceanography, 37, 1420-1433, 1992.

Brix, H., Sorrell, B. K., and Lorenzen, B.: Are Phragmites-dominated wetlands a net source or net sink of greenhouse gases?, Aquatic Botany, 69, 313-324, 2001.

Burdige, D.: Estuarine and coastal sediments–coupled biogeochemical cycling, Treatise on Estuarine and Coastal Science, 5, 279-316, 2012.

Burton, E., Bush, R. T., Johnston, S. G., Sullivan, L. A., and Keene, A. F.: Sulfur biogeochemical cycling and novel Fe–S mineralization pathways in a tidally re-flooded wetland, Geochimica et Cosmochimica Acta, 75, 3434-3451, 2011.

Burton, E. D., Bush, R. T., and Sullivan, L. A.: Elemental sulfur in drain sediments associated with acid sulfate soils, Applied Geochemistry, 21, 1240-1247, 2006.

Burton, E. D., Bush, R. T., Sullivan, L. A., and Mitchell, D. R. G.: Reductive transformation of iron and sulfur in schwertmannite-rich accumulations associated with acidified coastal lowlands, Geochimica et Cosmochimica Acta, 71, 4456-4473, 10.1016/j.gca.2007.07.007, 2007.

Cao, M., Gregson, K., and Marshall, S.: Global methane emission from wetlands and its sensitivity to climate change, Atmospheric environment, 32, 3293-3299, 1998.

Chanton, J. P., Arkebauer, T. J., Harden, H. S., and Verma, S. B.: Diel variation in lacunal CH 4 and CO 2 concentration and δ 13 C in Phragmites australis, Biogeochemistry, 59, 287-301, 2002.

Claff, S. R., Sullivan, L. A., Burton, E. D., and Bush, R. T.: A sequential extraction procedure for acid sulfate soils: partitioning of iron, Geoderma, 155, 224-230, 2010.

Clevering, O. A., and Lissner, J.: Taxonomy, chromosome numbers, clonal diversity and population dynamics of Phragmites australis, Aquatic Botany, 64, 185-208, 1999.

Conrad, R.: Mechanisms controlling methane emission from wetland rice fields, in: Biogeochemistry of Global Change, Springer, 317-335, 1993.

678 Costanza, R., de Groot, R., Sutton, P., van der Ploeg, S., Anderson, S. J., Kubiszewski, I.,
679 Farber, S., and Turner, R. K.: Changes in the global value of ecosystem services,
680 Global Environmental Change, 26, 152-158, 2014.
681 De La Cruz, A. A., and Hackney, C. T.: Enegry Value, Elemental Composition, and
682 Productivity of Belowground Biomass of a Juncus Tidal Marsh, Ecology, 58, 1165-
683 1170, 1977.
684 Deverel, S. J., Ingrum, T., and Leighton, D.: Present-day oxidative subsidence of organic
685 soils and mitigation in the Sacramento-San Joaquin Delta, California, USA,
686 Hydrogeology journal, 24, 569-586, 2016.
687 Finlayson, C. M., and Rea, N.: Reasons for the loss and degradation of Australian wetlands,
688 Wetlands Ecology and Management, 7, 1-11, 1999.
689 Freeman, C., Lock, M., and Reynolds, B.: Fluxes of CO_2, CH_4 and N_2O from a Welsh
690 peatland following simulation of water table draw-down: Potential feedback to climatic
691 change, Biogeochemistry, 19, 51-60, 1992.
692 Hemes, K. S., Chamberlain, S. D., Eichelmann, E., Knox, S. H., and Baldocchi, D. D.: A
693 biogeochemical compromise: The high methane cost of sequestering carbon in restored
694 wetlands, Geophysical Research Letters, 45, 6081-6091, 2018.
695 Henneberg, A., Sorrell, B. K., and Brix, H.: Internal methane transport through Juncus
696 effusus: experimental manipulation of morphological barriers to test above-and below-
697 ground diffusion limitation, New Phytologist, 196, 799-806, 2012.
698 Holmkvist, L., Ferdelman, T. G., and Jørgensen, B. B.: A cryptic sulfur cycle driven by iron
699 in the methane zone of marine sediment (Aarhus Bay, Denmark), Geochimica et
700 Cosmochimica Acta, 75, 3581-3599, 2011.
701 Jeffrey, L. C., Maher, D. T., Santos, I. R., McMahon, A., and Tait, D. R.: Groundwater, Acid
702 and Carbon Dioxide Dynamics Along a Coastal Wetland, Lake and Estuary Continuum,
703 Estuaries and Coasts, 39, 1325-1344, 2016.
704 Jeffrey, L. C., Maher, D. T., Johnston, S. G., Kelaher, B. P., Steven, A., and Tait, D. R.:
705 Wetland methane emissions dominated by plant-mediated fluxes: Contrasting
706 emissions pathways and seasons within a shallow freshwater subtropical wetland,
707 Limnology and Oceanography, 10.1002/lno.11158, 2019.
708 Johnston, S. G., Slavich, P. G., Sullivan, L. A., and Hirst, P.: Artificial drainage of
709 floodwaters from sulfidic backswamps: effects on deoxygenation in an Australian
710 estuary, Marine and Freshwater Research, 54, 781-795, 2003.

Johnston, S. G., Slavich, P. G., and Hirst, P.: The effects of a weir on reducing acid flux from a drained coastal acid sulphate soil backswamp, Agricultural Water Management, 69, 43-67, 2004.

Johnston, S. G., Keene, A. F., Burton, E. D., Bush, R. T., and Sullivan, L. A.: Quantifying alkalinity generating processes in a tidally remediating acidic wetland, Chemical Geology, 304, 106-116, 2012.

Johnston, S. G., Burton, E. D., Aaso, T., and Tuckerman, G.: Sulfur, iron and carbon cycling following hydrological restoration of acidic freshwater wetlands, Chemical Geology, 371, 9-26, 2014.

Karimian, N., Johnston, S. G., and Burton, E. D.: Acidity generation accompanying iron and sulfur transformations during drought simulation of freshwater re-flooded acid sulfate soils, Geoderma, 285, 117-131, 2017.

Karimian, N., Johnston, S. G., and Burton, E. D.: Iron and sulfur cycling in acid sulfate soil wetlands under dynamic redox conditions: A review, Chemosphere, 197, 803-816, 10.1016/j.chemosphere.2018.01.096, 2018.

Kim, J., Verma, S., Billesbach, D., and Clement, R.: Diel variation in methane emission from a midlatitude prairie wetland: significance of convective throughflow in Phragmites australis, Journal of Geophysical Research: Atmospheres, 103, 28029-28039, 1998.

Kirschke, S., Bousquet, P., Ciais, P., Saunois, M., Canadell, J. G., Dlugokencky, E. J., Bergamaschi, P., Bergmann, D., Blake, D. R., Bruhwiler, L., Cameron-Smith, P., Castaldi, S., Chevallier, F., Feng, L., Fraser, A., Heimann, M., Hodson, E. L., Houweling, S., Josse, B., Fraser, P. J., Krummel, P. B., Lamarque, J.-F., Langenfelds, R. L., Le Quéré, C., Naik, V., O'Doherty, S., Palmer, P. I., Pison, I., Plummer, D., Poulter, B., Prinn, R. G., Rigby, M., Ringeval, B., Santini, M., Schmidt, M., Shindell, D. T., Simpson, I. J., Spahni, R., Steele, L. P., Strode, S. A., Sudo, K., Szopa, S., van der Werf, G. R., Voulgarakis, A., van Weele, M., Weiss, R. F., Williams, J. E., and Zeng, G.: Three decades of global methane sources and sinks, Nature Geoscience, 6, 813-823, 10.1038/ngeo1955, 2013.

Knorr, K.-H., Glaser, B., and Blodau, C.: Fluxes and 13 C isotopic composition of dissolved carbon and pathways of methanogenesis in a fen soil exposed to experimental drought, Biogeosciences Discussions, 5, 1319-1360, 2008.

Konnerup, D., Sorrell, B. K., and Brix, H.: Do tropical wetland plants possess convective gas flow mechanisms?, New Phytol, 190, 379-386, 10.1111/j.1469-8137.2010.03585.x, 2011.

Lal, R.: Carbon sequestration, Philosophical Transactions of the Royal Society of London B: Biological Sciences, 363, 815-830, 2008.

Melton, J., Wania, R., Hodson, E., Poulter, B., Ringeval, B., Spahni, R., Bohn, T., Avis, C., Beerling, D., and Chen, G.: Present state of global wetland extent and wetland methane modelling: conclusions from a model intercomparison project (WETCHIMP), Biogeosciences, 10, 753-788, 2013.

Milberg, P., Tornqvist, L., Westerberg, L. M., and Bastviken, D.: Temporal variations in methane emissions from emergent aquatic macrophytes in two boreonemoral lakes, AoB Plants, 9, plx029, 10.1093/aobpla/plx029, 2017.

Mitsch, W. J., Bernal, B., Nahlik, A. M., Mander, Ü., Zhang, L., Anderson, C. J., Jørgensen, S. E., and Brix, H.: Wetlands, carbon, and climate change, Landscape Ecology, 28, 583-597, 2013.

Moore, G. E., Burdick, D. M., Peter, C. R., and Keirstead, D. R.: Belowground biomass of Phragmites australis in coastal marshes, Northeastern Naturalist, 19, 611-627, 2012.

Mulvey, P.: Pollution, prevention and management of sulphidic clays and sands. Proceedings National Conference on Acid Sulphate Soils. (Ed. R Bush) pp, 116-129, 1993.

Nedwell, D. B., and Watson, A.: CH4 production, oxidation and emission in a UK ombrotrophic peat bog: influence of SO42− from acid rain, Soil Biology and Biochemistry, 27, 893-903, 1995.

Neubauer, S. C., and Megonigal, J. P.: Moving beyond global warming potentials to quantify the climatic role of ecosystems, Ecosystems, 18, 1000-1013, 2015.

Page, K., and Dalal, R.: Contribution of natural and drained wetland systems to carbon stocks, CO2, N2O, and CH4 fluxes: an Australian perspective, Soil Research, 49, 377-388, 2011.

Pangala, S. R., Enrich-Prast, A., Basso, L. S., Peixoto, R. B., Bastviken, D., Hornibrook, E. R., Gatti, L. V., Marotta, H., Calazans, L. S. B., and Sakuragui, C. M.: Large emissions from floodplain trees close the Amazon methane budget, Nature, 552, 230, 2017.

Penhale, P. A., and Wetzel, R. G.: Structural and functional adaptations of eelgrass (Zostera marina L.) to the anaerobic sediment environment, Canadian Journal of Botany, 61, 1421-1428, 1983.

Pereyra, A. S., and Mitsch, W. J.: Methane emissions from freshwater cypress (Taxodium distichum) swamp soils with natural and impacted hydroperiods in Southwest Florida, Ecological Engineering, 114, 46-56, 2018.

778 Petrescu, A. M., Lohila, A., Tuovinen, J. P., Baldocchi, D. D., Desai, A. R., Roulet, N. T.,
779 Vesala, T., Dolman, A. J., Oechel, W. C., Marcolla, B., Friborg, T., Rinne, J.,
780 Matthes, J. H., Merbold, L., Meijide, A., Kiely, G., Sottocornola, M., Sachs, T., Zona,
781 D., Varlagin, A., Lai, D. Y., Veenendaal, E., Parmentier, F. J., Skiba, U., Lund, M.,
782 Hensen, A., van Huissteden, J., Flanagan, L. B., Shurpali, N. J., Grunwald, T.,
783 Humphreys, E. R., Jackowicz-Korczynski, M., Aurela, M. A., Laurila, T., Gruning,
784 C., Corradi, C. A., Schrier-Uijl, A. P., Christensen, T. R., Tamstorf, M. P.,
785 Mastepanov, M., Martikainen, P. J., Verma, S. B., Bernhofer, C., and Cescatti, A.:
786 The uncertain climate footprint of wetlands under human pressure, Proc Natl Acad Sci
787 U S A, 112, 4594-4599, 10.1073/pnas.1416267112, 2015.
788 Pfeifer-Meister, L., Gayton, L. G., Roy, B. A., Johnson, B. R., and Bridgham, S. D.:
789 Greenhouse gas emissions limited by low nitrogen and carbon availability in natural,
790 restored, and agricultural Oregon seasonal wetlands, PeerJ, 6, 10.7717/peerj.5465,
791 2018.
792 Poffenbarger, H. J., Needelman, B. A., and Megonigal, J. P.: Salinity influence on methane
793 emissions from tidal marshes, Wetlands, 31, 831-842, 2011.
794 Postma, D., and Jakobsen, R.: Redox zonation: equilibrium constraints on the Fe (III)/SO4-
795 reduction interface, Geochimica et Cosmochimica Acta, 60, 3169-3175, 1996.
796 Rayment, G., and Higginson, F. R.: Australian laboratory handbook of soil and water
797 chemical methods, Inkata Press Pty Ltd, 1992.
798 Sammut, J., White, I., and Melville, M.: Acidification of an estuarine tributary in eastern
799 Australia due to drainage of acid sulfate soils, Marine and Freshwater Research, 47,
800 669-684, 1996.
801 Saunois, M., Bousquet, P., Poulter, B., Peregon, A., Ciais, P., Canadell, J. G., Dlugokencky,
802 E. J., Etiope, G., Bastviken, D., and Houweling, S.: The global methane budget 2000–
803 2012, Earth System Science Data (Online), 8, 2016.
804 Sivan, O., Antler, G., Turchyn, A. V., Marlow, J. J., and Orphan, V. J.: Iron oxides stimulate
805 sulfate-driven anaerobic methane oxidation in seeps, Proceedings of the National
806 Academy of Sciences, 111, E4139-E4147, 2014.
807 Sorrell, B. K., and Boon, P. I.: Convective gas flow in Eleocharis sphacelata R. Br.: methane
808 transport and release from wetlands, Aquatic Botany, 47, 197-212, 1994.
809 Tucker, G. C.: The genera of Arundinoideae (Gramineae) in the southeastern United States,
810 Journal of the Arnold Arboretum, 71, 145-177, 1990.

Tulau, M.: Acid Sulphate Soil Priority Management Areas on the Lower Hastings Camden Haven Floodplains, Department of Land and Water Conservation, 1999.

Villa, J. A., and Bernal, B.: Carbon sequestration in wetlands, from science to practice: An overview of the biogeochemical process, measurement methods, and policy framework, Ecological Engineering, 114, 115-128, 10.1016/j.ecoleng.2017.06.037, 2018.

Walker, P. H.: Seasonal and stratigraphic controls in coastal floodplain soils, Soil Research, 10, 127-142, 1972.

White, I., Melville, M., Wilson, B., and Sammut, J.: Reducing acidic discharges from coastal wetlands in eastern Australia, Wetlands Ecology and Management, 5, 55-72, 1997.

Whiting, G. J., and Chanton, J. P.: Plant-dependent CH4 emission in a subarctic Canadian fen, Global biogeochemical cycles, 6, 225-231, 1992.

Whiting, G. J., and Chanton, J. P.: Greenhouse carbon balance of wetlands: methane emission versus carbon sequestration, Tellus B: Chemical and Physical Meteorology, 53, 521-528, 2001.

Wang, Z., Zeng, D., and Patrick, W. H.: Methane emissions from natural wetlands, Environmental Monitoring and Assessment, 42, 143-161, 1996.

Wong, V. N., Johnston, S. G., Bush, R. T., Sullivan, L. A., Clay, C., Burton, E. D., and Slavich, P. G.: Spatial and temporal changes in estuarine water quality during a post-flood hypoxic event, Estuarine, Coastal and Shelf Science, 87, 73-82, 2010.